

Cross Sections for the ${}^7\text{Be}(p, \gamma){}^8\text{B}$ Reaction*

F. J. Vaughn, R. A. Chalmers, D. Kohler, and L. F. Chase, Jr.
Lockheed Palo Alto Research Laboratory, Palo Alto, California 94304
 (Received 13 July 1970)

Cross sections for the ${}^7\text{Be}(p, \gamma){}^8\text{B}$ reaction have been measured at 20 proton energies ranging from 0.953 to 3.281 MeV. Measurements were made relative to the cross section for the ${}^7\text{Li}(d, p){}^8\text{Li}$ reaction at the 0.770-MeV resonance peak. The results were analyzed in two ways to obtain values for $S(0)$, the zero-energy cross-section factor. The first type of analysis, based on the assumption that the observed cross section was composed of a non-resonant part and resonant contributions from the first two excited states of ${}^8\text{B}$, gave an $S(0)$ of 0.0263 ± 0.0027 keVb. The second type of analysis assumed an additional resonance contribution from a higher-lying state and led to an $S(0)$ of 0.0226 ± 0.0043 keVb. The result obtained from the second analysis represents our best estimate for the value of $S(0)$ obtainable from the present measurements.

I. INTRODUCTION

A rare mode of termination of the p - p chain of hydrogen-burning reactions in the sun proceeds through the ${}^7\text{Be}(p, \gamma){}^8\text{B}$ radiative capture reaction. The ${}^8\text{B}$ produced subsequently decays by positron emission, primarily to the 2.90-MeV level of ${}^8\text{Be}$. In this decay a high-energy neutrino (end-point energy 14.06 MeV) is emitted. This sequence of reactions is so rare that the high-energy neutrinos carry only about 0.015% of the energy output of the sun.¹ However, because of the rapid rise with neutrino energy of the cross section for the ${}^{37}\text{Cl}(\nu, e^-){}^{37}\text{Ar}$ reaction, a large fraction of the observed counts in the solar-neutrino experiment of Davis, Harmer, and Hoffman² is expected to be produced by neutrinos emitted in the ${}^8\text{B}$ decay.³⁻⁵ This neutrino source is also expected to constitute an important factor in several other possible solar neutrino experiments (reviewed by Bahcall⁶). An accurate value for the ${}^7\text{Be}(p, \gamma){}^8\text{B}$ cross section at energies corresponding to the thermal energy of protons in the central regions of the sun (of the order of 15 keV) is therefore of crucial importance in predicting and interpreting the results of solar-neutrino experiments.

The results of measurements of the ${}^7\text{Be}(p, \gamma){}^8\text{B}$ cross section have previously been reported by Kavanagh⁷ and Parker.⁸⁻¹⁰ Both of these experimenters made measurements at relatively high proton energies (Kavanagh at 800 and 1400 keV, Parker at eight energies from 483 to 1932 keV) and analyzed their results with the aid of pertinent theoretical considerations^{11,12} to obtain the zero-energy cross-section factor, the quantity of principal astrophysical interest. Their reported cross-section factors, 0.021 ± 0.008 keVb (renormalized by Tombrello¹²) and 0.035 ± 0.004 keVb, respectively, disagree by about a factor of 2.

Because of the great importance of the ${}^7\text{Be}(p, \gamma){}^8\text{B}$ cross section, we have remeasured it, and have specifically extended the measurements to higher proton energies to investigate the effect of the second excited state of ${}^8\text{B}$ on the cross section. This state has been reported to be at an excitation energy of 2.17 ± 0.05 MeV by Dietrich, Honsaker, and Davies¹³ and at 2.34 ± 0.04 MeV by Brunnader, Hardy, and Cerny.¹⁴

II. EXPERIMENTAL PROCEDURES

The energy levels and decay schemes of the mass-8 nuclei pertinent to the present experiment are shown in Fig. 1. As previously indicated, ${}^8\text{B}$ nuclei produced by proton capture in ${}^7\text{Be}$ decay by positron emission to levels in ${}^8\text{Be}$. About 92.5%

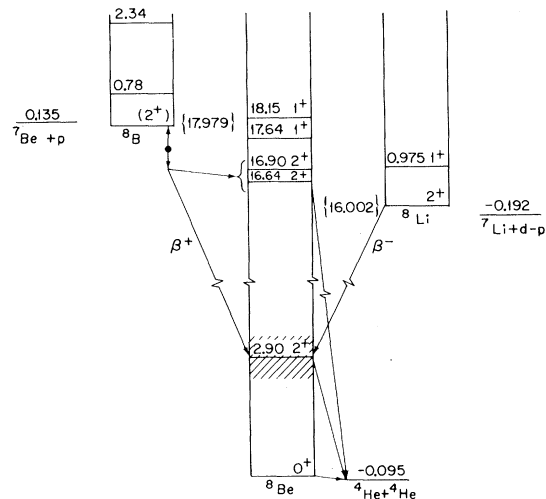


FIG. 1. Portion of level diagram for the $A=8$ triad pertinent to the reactions observed in the present experiment.

of the decays proceed through the broad 2.90-MeV state of ^8Be , with the remainder decaying to the 16.64- and 16.90-MeV states.¹⁵ Either of these decay modes is promptly followed by breakup into two α particles. As pointed out by Parker,⁸ these delayed α particles provide a unique signature for the occurrence of the $^7\text{Be}(p, \gamma)^8\text{B}$ reaction. We therefore followed an experimental procedure similar to that of Parker, in that we counted these delayed α particles to determine the occurrence of the desired reaction.

The ^7Be target was prepared by first passing a $^7\text{BeCl}$ solution containing about 22 mCi of ^7Be through an ion-exchange column to remove the major impurities. The concentrated solution was then deposited on a platinum backing and dried by heating to about 150°C. The final target spot was roughly rectangular in shape, with dimensions about 2.8 by 4.6 mm.

The incident proton beam was produced by the Lockheed 3-MV Van de Graaff accelerator. The beam was first passed through crossed magnetic and electric fields to insure that no particles other than protons were present. It then passed between sets of horizontal and vertical parallel plates to which triangular-shaped voltage waveforms of in-

commensurate frequencies were applied. The maximum amplitudes of these voltages were adjusted at each proton energy so that the beam was swept across the target spot both vertically and horizontally, covering substantially the same area of the target at each energy. Thus any effects due to nonuniformity of the ^7Be density over the target spot were minimized.

The experimental geometry in the region near the target is shown in Fig. 2. The beam passes through a collimating diaphragm which is maintained at +180 V to suppress escape of electrons. It then passes through an aperture in the cylindrical cup shown in the figure and hits the target. The target and cup assembly are electrically connected; measurement of the current on the target provides an accurate monitor of the incident positive beam, since essentially all electrons knocked out of the target are collected by the cup.

The target itself is mounted on a rotatable support as shown; during bombardment it is in the orientation indicated in the figure, and is rotated 90° to a position in front of the detector for counting. The bombard-count cycle was computer-controlled. The timing of the various portions of the cycle was as follows: bombardment, 1 sec; transfer to count position, 0.25 sec (the actual transfer took 100–150 msec); count, 1.2 sec; transfer back to irradiate position, 0.6 sec. The beam was deflected off the target except during the irradiate portion of the cycle. The count portion of the cycle was also automatically controlled by computer so that 30 successive spectra were obtained after each bombardment, each spectrum being collected for a period of 40 msec. Thus the time behavior of the beam-induced activity was followed.

The detector was a totally depleted Si surface-barrier solid-state counter. It had an active area of about 32 mm² and a thickness of $23 \pm 6 \mu\text{m}$, which is sufficient to stop α particles with energies up to about 6 MeV. The spectrum of α particles emitted in the decay of ^8Be extends to about 8.5 MeV. The fact that the higher-energy α particles did not stop in the detector did not, however, effect the measurements, since even 8.5-MeV α particles deposit about 3 MeV of energy in the detector, producing readily detectable pulses. The pulses made by positrons from the ^8B decay passing through the detector were only about 50 keV in height, and could be effectively biased out. Also, because of the small volume of the detector, only a moderate background was contributed by the 0.478-MeV γ rays emitted in the radioactive decay of ^7Be atoms in the target.

The experimental procedure employed in the actual cross-section measurements was essentially the same as that used by Parker.⁸ Namely, at

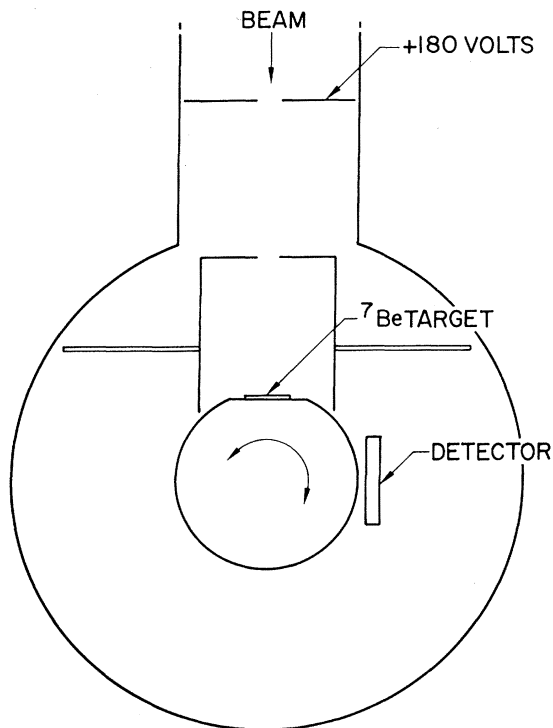


FIG. 2. Schematic diagram (horizontal section view) of the target chamber used for the $^7\text{Be}(p, \gamma)^8\text{B}$ cross-section experiment.

each proton energy the ratio of the cross section for the ${}^7\text{Be}(p, \gamma){}^8\text{B}$ reaction to that for the ${}^7\text{Li}(d, p){}^8\text{Li}$ reaction at the 0.770-MeV deuteron energy peak was measured. As is evident in the decay schemes shown in Fig. 1, the occurrence of both reactions can be detected by counting delayed α particles emitted in the breakup of the 2.90-MeV state of ${}^8\text{Be}$. Since the ${}^7\text{Be}$ of the target decays to ${}^7\text{Li}$, the sum of the numbers of ${}^7\text{Be}$ and ${}^7\text{Li}$ nuclei remains constant. This makes it possible to measure the ratio of the density of ${}^7\text{Be}$ nuclei in the target to the ${}^7\text{Li}$ density by using the observed delayed α yields from deuteron and proton bombardments. In practice, deuteron bombardments were made both before and after each proton bombardment. The ${}^7\text{Be}(p, \gamma){}^8\text{B}$ cross section can then be determined from the relative yields of delayed α particles from the ${}^7\text{Li}(d, p){}^8\text{Li}$ and ${}^7\text{Be}(p, \gamma){}^8\text{B}$ reactions, together with the absolute cross section for the former at the peak of the 0.770-MeV resonance. The value used for this peak cross section was 193 ± 18 mb, which is a weighted average of the two most accurate reported values, namely, those of Kavanagh⁷ and Parker.⁸

The appropriate expression for the ${}^7\text{Be}(p, \gamma){}^8\text{B}$ cross section is

$$\sigma_{8\text{B}} = 1.020\sigma_{8\text{Li}} \frac{\Delta Q_d}{\Delta Q_p} \frac{Y_{8\text{B}}(t_1)}{Y_{8\text{Li}}(t_2) - Y_{8\text{Li}}(t_0)} \times [e^{-\lambda(t_0-t_1)} - e^{-\lambda(t_2-t_1)}],$$

where the ΔQ 's are the amounts of charge collected on the target during deuteron and proton bombardments, the Y 's are the yields of delayed α particles following the decay of ${}^8\text{B}$ or ${}^8\text{Li}$, λ is the decay constant of ${}^7\text{Be}$, $\sigma_{8\text{Li}}$ is the cross section for ${}^7\text{Li}(d, p){}^8\text{Li}$ at the 0.770-MeV resonance peak (averaged over the target thickness), and the numerical factor (1.020) arises because of the difference in the half-lives of ${}^8\text{Li}$ (0.849 sec) and ${}^8\text{B}$ (0.774 sec). The times t_0 , t_1 , and t_2 are the time of target preparation, time of proton bombardment, and time of deuteron bombardment, respectively.

An analysis of the results of the deuteron bombardments indicated that the ratio of the number of ${}^7\text{Li}$ atoms in the target to the number of ${}^7\text{Be}$ atoms at the time the target was made ($t = t_0$) was -0.028 ± 0.047 . Since this number cannot be negative, it was assumed to be zero, which implies that $Y_{8\text{Li}}(t_0)$ in the cross-section formula is zero. The analysis of the deuteron bombardments referred to above included the effects produced by a slow loss of target material during the course of the bombardments. The amount of this loss was obtained by counting the 0.478-MeV γ rays emitted in the ${}^7\text{Be}$ decay as a function of time and compar-

ing the observed counting rates with those predicted from the known half-life of the decay.

In order to determine the target thickness, a series of deuteron bombardments was made in which the deuteron energy was varied over the region encompassing the 0.770-MeV resonance. The observed yield of delayed α particles as a function of energy was compared with calculated yield curves obtained using the known shape of the ${}^7\text{Li}(d, p){}^8\text{Li}$ cross section. From this comparison the target thickness was found to be 0.40 ± 0.05 mg/cm². (Only a small fraction of this thickness was composed of Li and Be, the rest probably being hydrocarbons from the ion-exchange resin, oxygen, chlorine, and other impurities.)

An extensive series of measurements was also made to determine the background counting rate. Three types of background runs were made. First, the beam-off, time-dependent background was obtained by operating the counter through its normal cycle for many thousands of cycles with the target in the chamber but with no beam. Second, the normal cycle was run but with a proton beam bombarding a gold foil rather than the Be target. Finally, a measurement of the amount of deuteron contamination of the proton beam, which would produce counts on the ${}^7\text{Li}$ component of the target during proton bombardments, was made by bombarding a thin Li target alternately with protons and deuterons and comparing the observed counting rates. The results of these three types of background runs indicated that only the time-dependent background was significant; this type of background was found to contribute 0.321 ± 0.097 counts per 1000 cycles to the observed rates. This was less than 10% of the observed counting rate over most of the energy range in which cross sections were measured. It was most significant at the lowest energies, and constituted about 25% of the observed counting rate at the lowest-energy point.

Cross-section measurements were made at 20 energies ranging from 0.953 to 3.281 MeV. An attempt was made to obtain at least 200 counts at each energy, though somewhat lower numbers were obtained at the lowest energy [where the ${}^7\text{Be}(p, \gamma){}^8\text{B}$ cross section is the lowest] and at the highest energy (where the Van de Graaff beam was somewhat unstable). Since the observed counting rates during the proton bombardment were only about 3 to 15 per h, these bombardments were of many hours duration in order to obtain the desired number of counts.

The spectrum of delayed α particles obtained during a typical deuteron bombardment is shown in Fig. 3, while the sum of the spectra from all the proton bombardments is shown in Fig. 4. There is no observable difference in the shape of

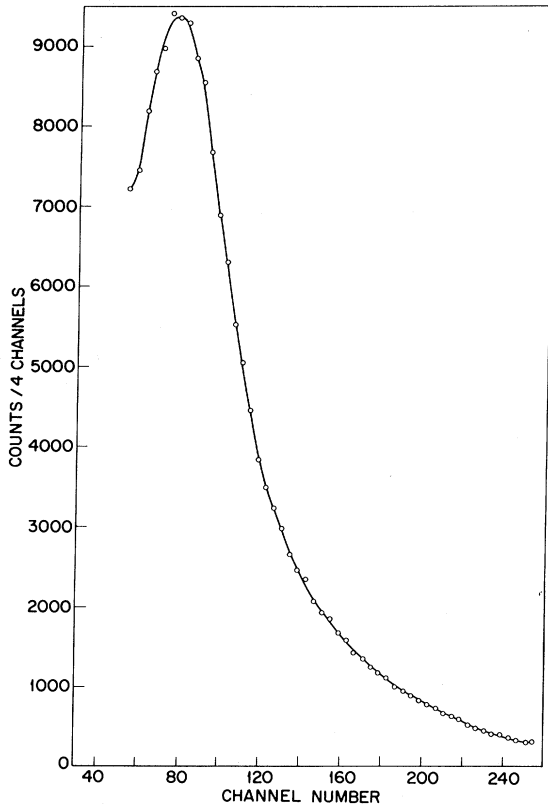


FIG. 3. Delayed- α -particle spectrum observed from decay of ^8Li produced by the $^7\text{Li}(d,p)^8\text{Li}$ reaction.

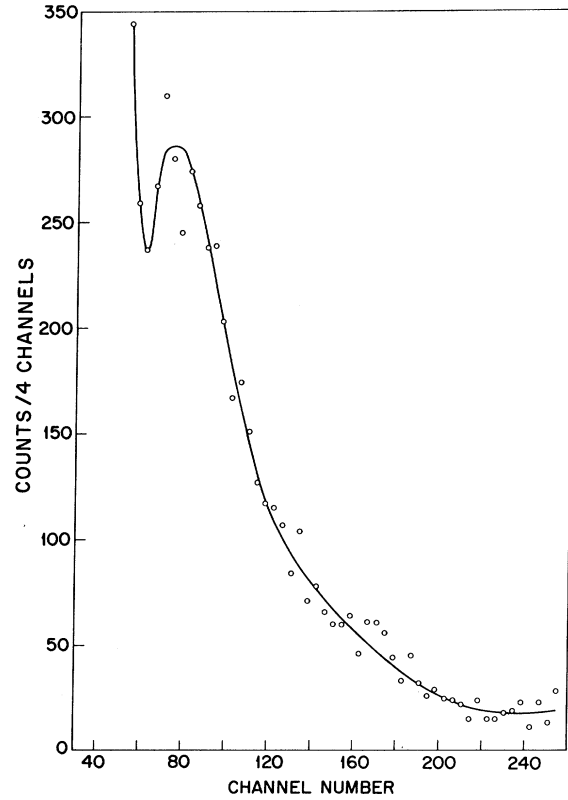


FIG. 4. Delayed- α -particle spectrum observed from decay of ^8B produced by the $^7\text{Be}(p,\gamma)^8\text{B}$ reaction.

these spectra, except for the low-energy tail present in the proton-run spectrum. This tail is produced by γ rays emitted in the decay of ^7Be atoms in the target. In obtaining the cross sections, only counts above this low-energy region were included, and the assumption was made that the same fraction of the spectra from deuteron and proton bombardments was included above the common energy threshold.

III. RESULTS AND CONCLUSIONS

The cross sections were calculated at each energy using the expression given previously, with the yield of ^8Li at $t=t_0$ taken to be zero. The results are listed in Table I, together with the relative and absolute uncertainties. Each cross section was calculated using the results of the deuteron runs immediately preceding and immediately following a proton bombardment; the listed values are an average of the two. At 1.056, 1.668, 2.476, and 2.678 MeV, two proton bombardments were made. The cross sections given at these energies are averages of the results from the two measurements. The absolute uncertainty in the average proton energy listed in the table was about 8 keV at the low-

TABLE I. Cross sections for the $^7\text{Be}(p,\gamma)^8\text{B}$ reaction.

E_p (MeV)	σ (μb)	$\Delta\sigma$ (rel.)	$\Delta\sigma$ (abs.)
0.953	0.570	0.057	0.073
1.056	0.508	0.092	0.10
1.158	0.625	0.054	0.073
1.261	0.636	0.056	0.075
1.465	0.862	0.074	0.10
1.668	1.000	0.060	0.078
1.871	1.039	0.078	0.11
2.073	1.08	0.10	0.13
2.174	1.36	0.10	0.15
2.275	1.40	0.10	0.15
2.375	1.58	0.13	0.18
2.476	1.84	0.15	0.22
2.577	1.81	0.15	0.21
2.678	1.58	0.14	0.20
2.778	1.98	0.17	0.23
2.879	1.48	0.12	0.17
2.979	1.57	0.15	0.19
3.080	1.56	0.13	0.18
3.180	1.84	0.17	0.22
3.281	1.80	0.23	0.27

est energy, decreasing smoothly to about 4 keV at the highest energy. These energy uncertainties were produced primarily by the uncertainties in target thickness and composition.

The relative uncertainties in the cross sections arose principally from the statistical uncertainties in the observed number of counts from the proton bombardments. In addition, an uncertainty of 3.1% was included because of the observed (nonstatistical) difference between yields at a particular energy obtained using the deuteron run results preceding and following the proton run. An uncertainty of the same amount was also included to allow for similar fluctuations in proton bombardment results, although such fluctuations were not observable because of the low counting rates. The absolute errors consist of the relative errors together with the uncertainty of the ${}^7\text{Li}(d, p){}^8\text{Li}$ cross section at the 0.770-MeV resonance peak and a small (about 1%) error arising from the effect of uncertainties in target thickness and composition. These target uncertainties produce an uncertainty in the ${}^7\text{Li}(d, p){}^8\text{Li}$ cross section averaged over the target thickness.

As indicated previously, the astrophysical significance of the ${}^7\text{Be}(p, \gamma){}^8\text{B}$ cross section depends on the value of the cross section near zero energy. For convenience, cross sections used in astrophysical applications are usually converted to the more nearly energy-independent S factor, which for the ${}^7\text{Be}(p, \gamma){}^8\text{B}$ reaction is given by

$$S(E) = 0.87441\sigma E e^{3.9734/E^{1/2}},$$

where E is the lab proton energy and σ is the cross section.

An analysis of the present cross-section results was carried out to obtain the zero-energy cross-section factor. In making such an analysis, one must make some assumptions concerning the factors which contribute to the observed cross sections. The value of the resulting zero-energy cross-section factor will depend, at least to some extent, on these assumptions. We have carried out analyses based on two general assumptions concerning the various components which contribute to the observed cross sections.

The first analysis leads to a zero-energy cross-section factor which can be directly compared with those of Kavanagh⁷ and Parker.^{8,10} This analysis was based on the assumption that the measured cross section was composed of a nonresonant part plus resonant contributions from the first and second excited states of ${}^8\text{B}$. The shape of the nonresonant part in the energy region up to 1.5 MeV was assumed to be that given by Tombrello¹²; above 1.5 MeV, this shape was obtained from a linear ex-

trapolation of Tombrello's cross-section-factor curve.¹⁶ The magnitude of the nonresonant cross section was treated as an adjustable parameter (as by Parker⁹). The resonance parameters for the first excited state of ${}^8\text{B}$ were taken from the work of Parker,⁹ while the proton width, γ width, and resonance energy of the second excited state were treated as adjustable parameters. The second excited state of ${}^8\text{B}$ was assumed to be a 3^+ state analogous to the corresponding state in ${}^8\text{Li}$, and was therefore assumed to be excited by p -wave protons. Its proton width was expressed as a function of the penetrability, the γ width was assumed to vary as the third power of the excitation energy, and the shift factor was included in the expression for the cross section produced by this resonance.

The best least-squares values of the four adjustable parameters, together with their uncertainties, were then obtained from the results of a computer calculation, using a generalized least-squares code. The fit to the experimental data was reasonably good, as indicated by a normalized χ^2 of about 1.24. The results of this analysis are shown in Fig. 5. The solid curve shows the calculated total cross section, while the three individual cross-section components are indicated by the other curves. The curve which extends down to an energy near zero is the renormalized Tombrello nonresonant cross section. The best-fit value for the resonance energy of the second excited state of ${}^8\text{B}$ was found to be 2.389 ± 0.072 MeV, in good agreement with the value of 2.34 ± 0.04 MeV reported by Brunnader, Hardy, and Cerny.¹⁴ However, the value obtained for the proton width of this resonance, 1.28 ± 0.44 MeV, is much larger than the 390 ± 40 keV previously reported.¹⁷

The normalization to Tombrello's S -factor curve

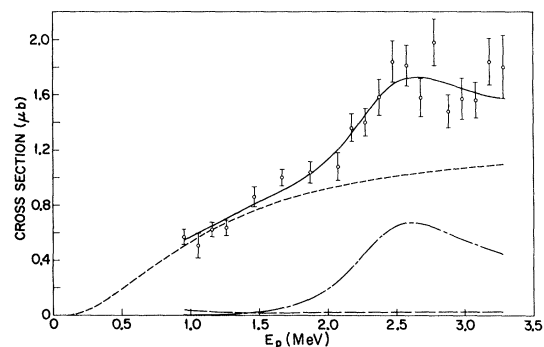


FIG. 5. Measured cross sections for the ${}^7\text{Be}(p, \gamma){}^8\text{B}$ reaction and best theoretical curve (solid curve) using first type of analysis (see text). Solid curve is the sum of: — — nonresonant part of the cross section, — — resonant cross section from the 0.78-MeV resonance, and - - - resonant cross section from the 2.34-MeV resonance.

gives a value of 0.0263 ± 0.0027 keV b for the zero-energy intercept. The uncertainty includes all known sources of experimental error, including the uncertainty in the ${}^7\text{Li}(d,p){}^8\text{Li}$ cross section, but no attempt has been made to assess the possible error in the shape of Tombrello's S-factor curve, and no uncertainty is included to take such an error into account. These values for the zero-energy intercept and its uncertainty are, of course, dependent on the assumption that the cross section is composed of the three components included in this analysis with no significant contribution from any other component.

The S-factor curve obtained from this fit to the cross-section data is shown in Fig. 6. The points plotted in the figure were obtained from the measured cross sections by subtracting the resonant contributions and then converting the remainder to cross-section factors, while the uncertainties shown are intended to indicate only the relative reliability of the points.

A weighted average value of $S(0)$, the zero-energy cross-section factor, has been calculated using the values obtained from the analysis presented above for the present experiment together with the results of Kavanagh and Parker. Kavanagh's cross sections were first adjusted by renormalizing to the weighted average value of 193 mb for the ${}^7\text{Li}(d,p){}^8\text{Li}$ cross section, subtracting the resonant contributions, and including a correction for the fraction of the ${}^8\text{B}$ decays which proceed through the 16.64- and 16.90-MeV pair of states in ${}^8\text{Be}$. This fraction of the decays was not measured by Kavanagh's method, but it did contribute to the measured cross section in our work and that of Parker; the fraction¹⁵ was taken to be 0.075. Kavanagh's nonresonant cross sections were then renormalized to Tombrello's results rather than

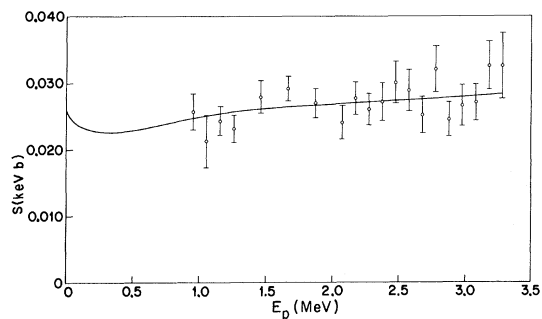


FIG. 6. Cross-section factor S for the ${}^7\text{Be}(p,\gamma){}^8\text{B}$ reaction as a function of proton energy, obtained from the fit of Fig. 5. Solid curve obtained from calculated nonresonant portion of the cross section; points obtained from measured cross sections reduced by calculated resonant contributions.

those of Christy and Duck¹¹ in order to have a consistent set of values from which to obtain an average. The adjusted value of $S(0)$ obtained in this way from Kavanagh's results was found to be 0.0222 ± 0.0063 keV b, where the uncertainty does not include that in the ${}^7\text{Li}(d,p){}^8\text{Li}$ cross section. Parker's value was taken to be 0.0348 ± 0.0015 keV b, where again the uncertainty in the ${}^7\text{Li}(d,p){}^8\text{Li}$ cross section is not included in the error. This value for Parker's $S(0)$ was obtained by calculating the weighted average of the ratio of the nonresonant cross-section factors given by Parker¹⁰ to the values from Tombrello's curve.¹² This weighted-average ratio was then applied to the zero-energy intercept of Tombrello. Our value of $S(0)$ used in obtaining the weighted average was 0.0263 ± 0.0012 keV b, where the uncertainty includes that obtained from the computer code fit for the normalization to Tombrello and the small errors arising from uncertainties in target thickness and composition. These three values of $S(0)$ were appropriately averaged, and the uncertainty of the ${}^7\text{Li}(d,p){}^8\text{Li}$ cross section was then included. The weighted average value of the zero-energy cross-section factor obtained in this way was found to be 0.0296 ± 0.0040 keV b. The uncertainty again does not include any possible error in the shape of Tombrello's S-factor curve.

It was mentioned earlier that the value of $S(0)$ obtained from the analysis of cross-section data depends to some extent on the assumptions employed, and that we have carried out analyses based on two general types of assumptions. The second type of analysis assumes that, in addition to the first two excited states of ${}^8\text{B}$, a higher-lying S-wave level also contributes to the observed cross section.

The second analysis was prompted by several factors. First, our results (see Fig. 5) show some evidence of a cross-section minimum at about 3 MeV, above which the cross section rises above the calculated value obtained using our first set of assumptions. Also, as indicated previously, the proton width of the second excited state of ${}^8\text{B}$ obtained from the least-squares fit to the data was much greater than that reported in the literature. Finally, recent measurements of the ${}^7\text{Be}(p,\gamma){}^8\text{B}$ cross section have been made by Kavanagh *et al.*¹⁸ over the energy region from about 150 keV to 10 MeV. Their preliminary results indicate that the nonresonant cross section calculated by Tombrello accounts for a continually decreasing fraction of the observed cross section as the energy increases.

We felt that the assumption that would best reflect the trend of our cross-section data in the region above 3 MeV and at the same time would be amenable to analysis was the inclusion of an S-wave level at an energy above 3 MeV. Essentially

the same least-squares computer code was then used to obtain the best values of the parameters. It proved impossible to obtain a fit with seven free parameters (the original four and three more for the additional resonance), so it was necessary to fix the values of some of them.

The results of various possibilities regarding the fixing of parameters were examined, but it was found that essentially all assumptions that we considered reasonable lead to quite similar results. The fits to the measured cross sections obtained from two typical cases are shown in Figs. 7 and 8. Both figures show the calculated total cross section as a solid curve, while the cross-section components are indicated by the other curves. (See figure captions.)

For the fit shown in Fig. 7, the resonance energy and proton width of the second excited state of ${}^8\text{B}$ were fixed at the best reported values, namely, 2.34 and 0.390 MeV, respectively, and the resonance energy of the higher-lying S-wave resonance was fixed at a lab energy of 3.8 MeV. The code then obtained the best least-squares values for the remaining four parameters. The normalized χ^2 for this fit was 0.91, indicating a considerably better fit than that obtained from the previous type of analysis. It was found that fits very similar to that shown in Fig. 7 were obtained with the S-wave resonance energy anywhere in the region from about 3.4 to 4.4 MeV. The magnitude of the nonresonant cross section, which is essentially the quantity of astrophysical interest, is quite insensitive to the value of this S-wave resonance energy. The value for $S(0)$ obtained from the fit of Fig. 7 is 0.0228 ± 0.0040 keV b, where again the un-

certainty does not include that in the ${}^7\text{Li}(d, p){}^8\text{Li}$ cross section. This is significantly lower than the value (0.0263 ± 0.0027) obtained with the first type of analysis, essentially because the effect of the S-wave resonance extends over the entire energy range in which measurements were made. The greater uncertainty than that obtained with the first type of analysis is a reflection of the fact that, with more parameters available, changes in the value of the nonresonant cross section can more readily be compensated for by changes in the values of other parameters. It should perhaps be noted that the γ -ray width of the second excited state of ${}^8\text{B}$ obtained from the fit of Fig. 7 is very close to that predicted from the γ width of the corresponding state in ${}^8\text{Li}$, the mirror nucleus of ${}^8\text{B}$.

The fit shown in Fig. 8 was also obtained with the resonance energy and width of the second excited state of ${}^8\text{B}$ fixed at their best reported values and the S-wave resonant energy fixed at 3.8 MeV in the lab system. In addition, the γ -ray width of this state was fixed at half the value obtained from that of the corresponding mirror-nucleus state. This last assumption was made essentially to reduce the magnitude of the P-wave resonant peak and determine whether a reasonable fit could still be obtained consistent with both our data and the results of the recent measurements of Kavanagh *et al.*,¹⁸ which show only a small resonance peak. The fit obtained was nearly as good as that for the case shown in Fig. 7, as reflected by a normalized χ^2 of 1.05. The value of $S(0)$ corresponding to the fit of Fig. 8 is 0.0225 ± 0.0035 keV b, where again the uncertainty does not include that in the ${}^7\text{Li}(d, p){}^8\text{Li}$ cross section.

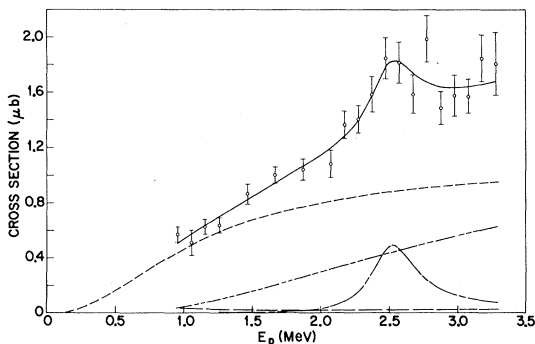


FIG. 7. Measured cross sections for the ${}^7\text{Be}(p, \gamma){}^8\text{B}$ reaction and typical theoretical fit (solid curve) from second type of analysis (see text). Solid curve is sum of: — — — nonresonant part of the cross section, — — — resonant cross section from the 0.78-MeV resonance, — · — · — resonant cross section from the 2.34-MeV resonance, and — — — resonant cross section from an s-wave level at 3.8 MeV (lab energy).

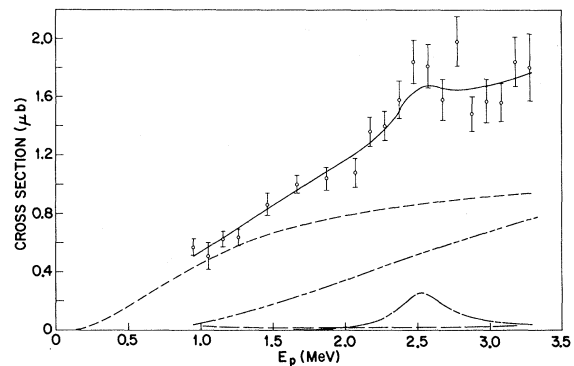


FIG. 8. Measured cross sections for the ${}^7\text{Be}(p, \gamma){}^8\text{B}$ reaction and typical theoretical fit (solid curve) from second type of analysis (see text). Solid curve is sum of: — — — nonresonant part of the cross section, — — — resonant cross section from the 0.78-MeV resonance, — · — · — resonant cross section from the 2.34-MeV resonance (with γ width fixed at about half that used in fit of Fig. 7), and — — — resonant cross section from an s-wave level at 3.8 MeV (lab energy).

The S -factor curve obtained from the fit of Fig. 7 is indicated in Fig. 9. It should be noted that the corresponding curve for the case shown in Fig. 8 would be insignificantly different. As for the previous S -factor curve, the points were obtained by converting the nonresonant portion of the cross sections to S factors, and the uncertainties indicate the relative reliability of the points.

It is felt that the assumptions made in the second type of analysis described above are perhaps physically more reasonable than those employed in the first type, and should therefore lead to a more reliable value for $S(0)$. Therefore, we feel that the best value for the zero-energy cross-section factor obtainable from our cross-section data is 0.0226 ± 0.0043 keV b. This is an average of the values calculated from the fits shown in Figs. 7 and 8, and the uncertainty quoted includes that in the ${}^7\text{Li}(d, p){}^8\text{Li}$ peak cross section. In general, it should be pointed out that considerations such as those brought out in our second type of analysis, which indicate that nonresonant capture may not account for all the observed cross section even at relatively low energies, must be taken into account in order to obtain an accurate value of $S(0)$ from cross-section data.

We have made no attempt to carry out a detailed reanalysis of Kavanagh's and Parker's results using the assumptions made in our second type of analysis. However, if one assumes that the weighted average values of $S(0)$ for the three experiments are the same fraction of our result as those found previously, one obtains a value for $S(0)$ of 0.0254 ± 0.0048 keV b, where the fractional uncertainty was taken to be the same as that found in our result.

Previously reported values of $S(0)$, the values obtained from the two types of analysis of our re-

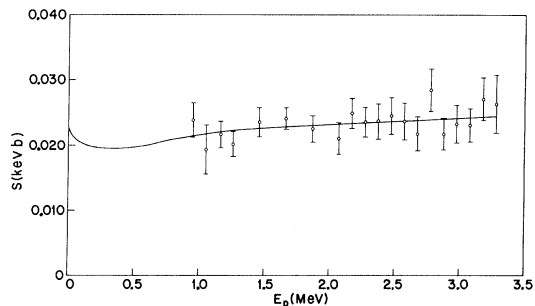


FIG. 9. Cross-section factor S for the ${}^7\text{Be}(p, \gamma){}^8\text{B}$ reaction as a function of proton energy, obtained from the fit of Fig. 7. Solid curve obtained from calculated nonresonant portion of the cross section; points obtained from measured cross sections reduced by calculated resonant contributions.

TABLE II. Zero-energy cross-section factor for the ${}^7\text{Be}(p, \gamma){}^8\text{B}$ reaction.

$S(0) \pm \Delta S(0)$	Explanation
0.021 ± 0.008	Value reported by Kavanagh, renormalized by Tombrello. ^a
0.035 ± 0.004	Corrected value reported by Parker. ^b
0.0263 ± 0.0027	Obtained from present measurements using first type of analysis.
0.0226 ± 0.0043	Obtained from present measurements using second type of analysis.
0.0296 ± 0.0040	Weighted average value using results from present experiment, Kavanagh, Parker, and first type of analysis.
0.0254 ± 0.0048	Weighted average value using results from present experiment, Kavanagh, Parker, and second type of analysis.

^aSee Ref. 7, renormalized in Ref. 12.

^bSee Ref. 10.

sults, and the corresponding weighted averages using the results of Kavanagh, Parker, and the present experiment are collected for convenience in Table II.

Using the weighted average values for the cross-section factor obtained from our two methods of analysis, predicted counting rates for the solar-neutrino experiment of Davis, Harmer, and Hoffman can be obtained. The rate of neutrino capture is (from calculations given in Ref. 4)

$$1.3 + 5.8 \frac{S(0)}{0.043} (1 \pm 0.4) \text{ SNU},$$

where $S(0)$ is the zero-energy cross-section factor for ${}^7\text{Be}(p, \gamma){}^8\text{B}$, the coefficient multiplying $S(0)$ has been corrected to incorporate later results,¹⁹ the quoted error is an approximate upper limit to the uncertainty,⁴ and the result is expressed in solar-neutrino units ($1 \text{ SNU} = 10^{-36}$ capture per target particle per sec). Inserting our weighted average values for $S(0)$ gives $5.3 \pm 2.1 \text{ SNU}$ and $4.7 \pm 1.9 \text{ SNU}$ as the predicted neutrino capture rates in the Davis, Harmer, and Hoffman experiment, based on the first and second types of analysis, respectively. These are to be compared with an experimental upper limit of 3 SNU reported by Davis, Harmer, and Hoffman.² The predicted values and the reported upper limit are thus not in obvious disagreement, considering the magnitude of the uncertainties involved.

- *Work supported by the Office of Naval Research.
- ¹J. N. Bahcall and G. Shaviv, *Astrophys. J.* **153**, 113 (1968).
- ²R. Davis, Jr., D. S. Harmer, and K. C. Hoffman, *Phys. Rev. Letters* **20**, 1205 (1968).
- ³J. N. Bahcall, *Phys. Rev.* **135**, B137 (1964).
- ⁴J. N. Bahcall, N. A. Bahcall, and G. Shaviv, *Phys. Rev. Letters* **20**, 1209 (1968).
- ⁵J. N. Bahcall, N. A. Bahcall, and R. K. Ulrich, *Astrophys. J.* **156**, 559 (1969).
- ⁶J. N. Bahcall, *Phys. Rev. Letters* **23**, 251 (1969).
- ⁷R. W. Kavanagh, *Nucl. Phys.* **15**, 411 (1960).
- ⁸P. D. Parker, *Phys. Rev.* **150**, 851 (1966).
- ⁹P. D. Parker, *Astrophys. J.* **145**, 960 (1966).
- ¹⁰P. D. Parker, *Astrophys. J. Letters* **153**, L85 (1968).
- ¹¹R. F. Christy and I. Duck, *Nucl. Phys.* **24**, 89 (1961).
- ¹²T. A. Tombrello, *Nucl. Phys.* **71**, 459 (1965).
- ¹³F. S. Dietrich, J. L. Honsaker, and J. W. Davies, *Bull. Am. Phys. Soc.* **8**, 120 (1963).
- ¹⁴H. Brunnader, J. C. Hardy, and J. Cerny, *Phys. Rev.* **174**, 1247 (1968).
- ¹⁵E. Matt, H. Pfander, H. Rieseberg, and V. Soergel, *Phys. Letters* **9**, 174 (1964).
- ¹⁶T. A. Tombrello, private communication.
- ¹⁷R. L. McGrath, J. Cerny, and E. Norbeck, *Phys. Rev. Letters* **19**, 1442 (1967).
- ¹⁸R. W. Kavanagh, T. A. Tombrello, J. M. Mosher, and D. R. Goosman, *Bull. Am. Phys. Soc.* **14**, 1209 (1969).
- ¹⁹J. N. Bahcall and C. P. Moeller, *Astrophys. J.* **155**, 511 (1969).

Off-Shell Effects in Knockout Reactions*

Edward F. Redish, G. J. Stephenson, Jr., and Gerald M. Lerner
*Department of Physics and Astronomy and Center for Theoretical Physics,
 University of Maryland, College Park, Maryland 20742*
 (Received 24 July 1970)

The amplitude for a knockout reaction in the plane-wave impulse approximation is derived from the Faddeev equations. It factorizes into the product of an off-shell two-body t matrix times the bound-state wave function in momentum space. In this paper results are derived for the $(p, 2p)$ experiment from a realistic potential and compared with those arising from some current approximations. Distortion effects are ignored in order to isolate the off-shell effects. We find that for incident protons with lab energy below 200 MeV using an off-shell amplitude can change the cross section significantly as compared with the on-shell approximations in current use. The effect increases with the binding energy of the struck proton and with the recoil momentum. This indicates that $(p, 2p)$ reactions below 200 MeV are sensitive to the off-shell behavior of the two-body amplitude and that they should not be used to obtain nuclear information using on-shell approximations.

I. INTRODUCTION

Interest in knockout reactions which proceed via quasielastic scattering stems mainly from the two distinct kinds of information which may be extracted from them: (1) information about off-shell scattering amplitudes between the projectile and the struck particle, and (2) information about the wave function of the struck particle. Especially in $(p, 2p)$ reactions, most of the emphasis to date has been on the second type. In this paper, we focus on the off-shell information. Our understanding of these effects then allows us to discuss ambiguities in the extraction of the form factors and spectroscopic factors arising from off-shell properties.

Off-shell information may be obtained from many-body systems. It has been found that calculations of the density and binding energy of nuclear matter¹ and the low-energy three-nucleon proper-

ties² (H^3 binding energy and the doublet n - D scattering length) are very sensitive to the details of the two-nucleon force. Since these systems contain both protons and neutrons, their properties depend on both the $T=0$ and $T=1$ forces and are especially sensitive to the off-shell properties of both the 1S_0 and 3S_1 states and on the ratio of central to tensor forces. Because the nucleons interact over long periods of time and at low energies, the exclusion principle is important and must be taken into account in deriving the effective interactions.³ These facts make the extraction of off-shell information from the properties of bound many-body systems quite difficult.

Nuclear reactions provide an additional degree of freedom compared with bound states. Since continuum wave functions have flux at infinity, the investigator may choose a particular set of boundary conditions by specifying the incident particle, target, the energy of the reaction, etc. Comparisons